ELSEVIER

Journal of Molecular Catalysis A: Chemical 130 (1998) 261–269

JOURNAL OF MOLECULAR CATALYSIS A: CHEMICAL

Redox features of β-$VOPO_4$ catalyst using ^{18}O tracer and laser Raman spectroscopy

Hideo Numata, Takehiko Ono *

Department of Applied Chemistry, Osaka Prefecture University, 1-1 Gakuen-cho, Sakai, Osaka 593, Japan

Received 24 June 1997; accepted 26 September 1997

Abstract

The oxygen ions of the β-$VOPO_4$ catalyst were exchanged with an ^{18}O tracer by a reduction–oxidation method and by a catalytic oxidation of but-1-ene using $^{18}O_2$. The bands at 992 and 900 cm^{-1} were more shifted to lower frequencies than those at 1076 and 1002 cm^{-1}. Applying the correlation between the Raman bands and stretching vibrations in the literature, the exchanged oxygen species were estimated. The results suggest that the P–O–V vacancies corresponding to 992 and 900 cm^{-1} were responsible for reoxidation and the V=O oxygen corresponding to the 1002 cm^{-1} band of β-$VOPO_4$ was not. The $(VO)_2P_2O_7$ was oxidized to β-$VOPO_4$ by O_2 above 823 K. The insertion position of oxygen was determined at the bands at 992 and 900 cm^{-1} of β-$VOPO_4$ using $^{18}O_2$, which is the same as the exchanged position. © 1998 Elsevier Science B.V.

1. Introduction

Previously, we have investigated the Raman band shifts of MoO_3 [1], Mo mixed oxide [2] and V_2O_5 catalysts [3] exchanged with ^{18}O tracer via oxidation reactions. With the V_2O_5 catalyst [3], the band at 700 cm^{-1} was more shifted to lower frequencies than the band at 998 cm^{-1}. This suggested that the oxygen insertion from the gas phase takes place at the anion vacancies corresponding to the V–O band at 700 cm^{-1} in the V–O layer rather than those of the V=O band in the oxygen layer. With the MoO_3 catalyst, similar results were obtained [1].

The V–P–O catalysts has been used for oxidation of *n*-butane to maleic anhydride [4–8]. $(VO)_2P_2O_7$ has been specially indicated to be active phase for this oxidation. Schrader et al. [9–11] have studied these catalysts and the role of the oxygen species in the *n*-butane oxidation using β-$VOPO_4$ labeled with ^{18}O [11]. Koyano et al. [12,13] have studied the oxidation and reduction processes of the surface vanadyl pyrophosphate by means of Raman spectroscopy and XPS. Abdelouahab et al. [14,15] have studied various $VOPO_4$ catalysts using hydration and Raman spectroscopy methods. Zhang-Lin et al. [16,17] have reported activated VPO catalysts based vanadyl pyrophosphate. Assignments of Raman spectra in accordance with normal coordination analysis have not been reported for

* Corresponding author. Fax: +81-722-593340; e-mail: ono@chem.osakafu-u.ac.jp

PII S1381-1169(97)00217-3

these V–P–O oxides, but some empirical assignments have been attempted on β-$VOPO_4$ [11,18]. It is interesting to study which oxygen species are responsible for the β-$VOPO_4$ catalyst for the oxidation reactions though the selectivity to maleic anhydride is lower.

In this work the oxide ions of β-$VOPO_4$ were exchanged with an ^{18}O tracer via 1-butene oxidation. The Raman spectra of β-$VOPO_4$ partly exchanged with ^{18}O were registered and preferential shifts of the bands were compared. The oxidation of $(VO)_2P_2O_7$ by $^{16}O_2$ and $^{18}O_2$ was carried out and the Raman spectral changes with O_2 uptake were examined. The redox features of these catalysts were studied and the active sites for oxidation and reoxidation for β-$VOPO_4$ were discussed.

2. Methods

2.1. Preparation of catalysts

The β-$VOPO_4$ was prepared as follows [19]: 0.1 mol of H_3PO_4 was added to 0.1 mol NH_4VO_3 solution at 333 K. After evaporation on a water bath, the yellowish precursor was heated at 873 K for 10 h and then the β-$VOPO_4$ was obtained.

The $(VO)_2P_2O_7$ was prepared by two steps as follows [20,21]: firstly, the precursor $VO(HPO_4)\cdot 0.5H_2O$ was prepared. The desired amount of H_3PO_4 and V_2O_5 is mixed in the hydroxyl ammonium chloride ($(NH_3OH)Cl$) solution at 353 K for 1 h. The solution was kept at 403 K for 24 h. It changed to a paste state. Then it was boiled in water for 10 min. After filtration and washing, the greenish powder, i.e. the precursor $VO(HPO_4)\cdot 0.5H_2O$, was obtained. This phase was confirmed by X-ray diffraction as JPDSC 38-0291 and 37-0269. Secondly, the precursor was heated step by step to 823 K in a stream of nitrogen. After cooling, it was heated at 773 K in the presence of air for 2 h. The sample was washed by water and dried after filtration. Then $(VO)_2P_2O_7$ was obtained.

2.2. Procedures

The exchange of lattice oxygen of β-$VOPO_4$ catalysts with ^{18}O were performed by two methods. The first method is as follows: the mixture of 1-butene at ca. 4 kPa and $^{18}O_2$ (98.1 at%, Isotec) at ca. 1 kPa was reacted on the catalyst at 713 K using a circulation system (ca. 360 cm^3). The second method, a reduction–oxidation method, is as follows: the reduction of β-$VOPO_4$ catalysts by 1-butene was carried out at ca. 4 kPa and 700–750 K and the reoxidation by $^{18}O_2$ was carried out at the same temperature. The reaction products were buta-1,3-diene, CO, and CO_2, whose ^{18}O% were determined using a mass spectrometer (Shimadzu GCMS QP 2000A). The amount of ^{18}O exchanged in the β-$VOPO_4$ catalyst was assumed as those of ^{16}O in the products for the first method. For the second method, those were assumed to be the oxygen amount of the products in the reduction experiments. $(VO)_2P_2O_7$ was oxidized by $^{16}O_2$ and $^{18}O_2$ at 823–873 K using a circulation system. The percentage oxidized with O_2 was calculated using the following reaction: $(VO)_2P_2O_7 + \frac{1}{2}O_2 \rightarrow 2\,\beta$-$VOPO_4$.

The structure of catalysts was determined by the X-ray diffraction method using Cu Kα radiation and by laser Raman spectroscopy. The laser Raman spectra of the catalyst samples exchanged with ^{18}O were recorded on a JASCO NR-1000 laser Raman spectrometer. An Ar-ion laser was tuned to 514.5 nm for excitation. The laser power was set at 150–200 mW. The data were stored on a computer and the peak-shape analysis was carried out using the technique reported by Miyata et al. [22,23].

3. Results and discussion

3.1. Structure and Raman spectra of β-$VOPO_4$

The structure of β-$VOPO_4$ was investigated by some workers [24,25]. The structure model is

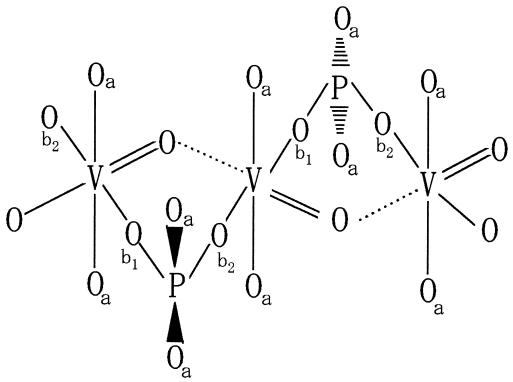

Fig. 1. Structure model of β-$VOPO_4$ [11].

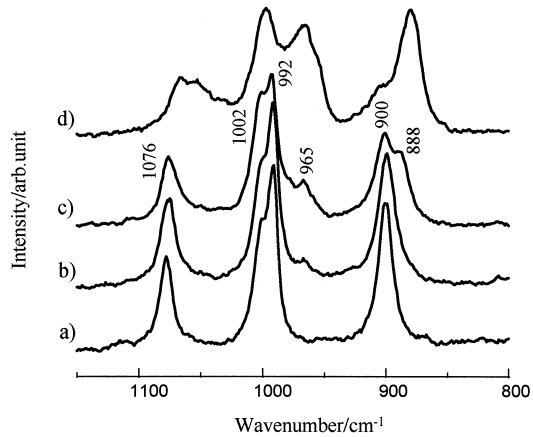

Fig. 2. Raman spectra of β-$VOPO_4$ exchanged with ^{18}O by a reduction–oxidation method (see Table 2). (a) no exchange; (b) 5 at% of oxygen exchanged; (c) 14%, and (d) well-exchanged β-$VOPO_4$, i.e., the reduction by 1-C_4H_8 and reoxidation by $^{18}O_2$ were repeated 5 times.

shown in Fig. 1. The VO_6 octahedra are linked with each other through V=O by a corner-sharing. The PO_4 tetrahedra are also linked with each V square oxygen by a corner-sharing. There are two kinds of P–O_b–V present and they have different distances (Table 1). There is one kind of P–O_a–V present across VO_6 chains as shown in Fig. 1 and Table 1.

Fig. 2a shows the Raman spectrum of β-$VOPO_4$. The bands at 1076, 1002, 992, and 900 cm^{-1} are obtained. The assignments were reported by Bhargava et al. [18] and Schrader et al. [11] as listed in Table 1. Bhargava et al. have assigned empirically the Raman bands at 1075 and 988 cm^{-1} to two asymmetric stretching P–O vibrations of phosphate ions. The bands at 1000 cm^{-1} and 900 cm^{-1} were assigned to the V=O and symmetric P–O stretches, respectively. On the other hand, Schrader et al. [11,26] have proposed that the vibration of phosphate ions around V octahedra is similar in magnitude and that the interactions between groups are probably comparable to those within groups. Then, they proposed the P–O_a–V and P–O_b–V stretching vibrations as shown in Table 1. The band at 1002 cm^{-1} is attributed to the V=O vibration as the same as that by Bhargava et al. The assignments by Schrader et al. have been adopted here. The discussion will be added later using our ^{18}O data in the oxidation of $(VO)_2P_2O_7$ in 3.5.

Table 1
Raman spectra of β-$VOPO_4$ and their assignments

Bhargava and Condrate [18]		Lashier and Schrader [11]		This work (cm^{-1})
mode	Raman band (cm^{-1})	mode	Raman band (cm^{-1})	
ν_{as}(P–O)	1075	P–O_a–V	1072	1076
ν(V=O)	999	V=O	998	1002
ν_{as}(P–O)	988	P–O_b–V	987	992
ν_s(P–O)	896	P–O_b–V	896	900

According to Gopal et al. [24] the distances of P–O_a and O_a–V for P–O_a–V are 1.528 and 1.886 Å, respectively. Two cases are present for P–O_b–V. In the first one P–O_{b1} and O_{b1}–V are 1.519 and 1.902 Å, respectively. In the second one P–O_{b2} and O_{b2}–V are 1.540 and 1.849 Å. That of V=O is 1.566 Å.

Table 2
Conversions of 1-butene, product selectivities and average ^{18}O exchange per cent over β-$VOPO_4$ catalyst at 713 K

Conversion of 1-C_4H_8 (%)	product selectivity (%)			Average ^{18}O exchange %
	C_4H_6	CO_2	CO	
5.2[a]	73	10	17	5
3.8	61	21	11	5
7.4	54	31	15	12
8.2	48	33	14	14
9.0	51	35	14	15
9.4[b]	59	9	32	2
22.8	47	27	26	5

[a] By a reduction–oxidation method at $p(1\text{-}C_4H_8) = 30$ Torr (1 Torr = 133.3 Pa), reaction time 15–35 min and 0.05 g of catalyst.
[b] By a catalytic oxidation method, $p(1\text{-}C_4H_8) = 16$ Torr, $p(^{18}O_2) = 9$ Torr, and reaction time 22–36 min.
The ^{18}O% in CO_2 is 35 and 29% for the conversions of 9.4% and 22.8%, respectively. The ^{18}O% in CO is 29 and 15% for conversions of 9.4% and 22.8%, respectively. The amounts of furan and maleic anhydride were not determined. The average, ^{18}O%, however, will be nearly the same as described above.

3.2. Oxygen exchange with ^{18}O over β-$VOPO_4$ catalysts

The catalysts were reduced with but-1-ene and were reoxidized with $^{18}O_2$ at the same temperature. The average exchange ^{18}O% in this case was listed in Table 2, which was calculated from the amounts of ^{16}O in the products, assuming that reoxidation of β-$VOPO_4$ by $^{18}O_2$ takes place completely. The catalyst oxygen ions were also exchanged with ^{18}O via catalytic oxidation using but-1-ene and $^{18}O_2$ over β-$VOPO_4$ catalysts. The conversion, product selectivity, and ^{18}O% in the products, and average exchange ^{18}O% in the β-$VOPO_4$ are also shown in Table 2. According to previous workers [9,10] furan as well as maleic anhydride were produced on this catalyst in butane oxidation. We have not determined the products here though they may be less produced. The average ^{18}O% of catalysts were calculated from the ^{16}O% of products such as CO, CO_2, and H_2O. The selectivity to buta-1,3-diene ranges at around 50–60% in both cases.

3.3. Raman band shifts of β-$VOPO_4$ catalysts exchanged with ^{18}O by a reduction–oxidation method

Fig. 2 shows the spectra of β-$VOPO_4$ before and after they were exchanged with ^{18}O. With the increase in ^{18}O exchange (Fig. 2a–c), the intensity of the band at 992 cm^{-1} decreases while that of the new 965 cm^{-1} band increases. The intensity of 900 cm^{-1} band decreases while that of the new ca. 880 cm^{-1} band increases. On the other hand, the bands at 1076 and 1002 cm^{-1} do not change so much in their intensities at low ^{18}O exchange. In this work, we could not observe the Raman spectrum after the reduction by but-1-ene. Moser et al. [10] have reported that the intensities of the bands at 987 (992) and 896 (902, this work) cm^{-1} decreased as compared to the intensity of the band at 1067 (1075) cm^{-1} in the butene oxidation at ca. 773 K, i.e. in the reduction conditions for the catalyst.

In order to know the shift change in details, the peak shape analysis was attempted with the spectra in Fig. 2 using Lorenzian function [22,23]. Fig. 3 shows the analysts for Fig. 2c. Good curve fittings are obtained when the spectrum consisted of 1075, 1050, 1002, 992, 977, 965, 900, and 888 cm^{-1}. It is thought that the bands at 888 are shifted from 900, 965 from 992, and 977 from 1002 cm^{-1}. The position of 977 cm^{-1} is not determined experimentally but is estimated in this fitting analysis. A new band shifted from 1076 cm^{-1} at low ^{18}O exchange is not detected (Fig. 2b). The shifted fractions with the 1002, 992 and 900 cm^{-1} bands are shown in Table 3.

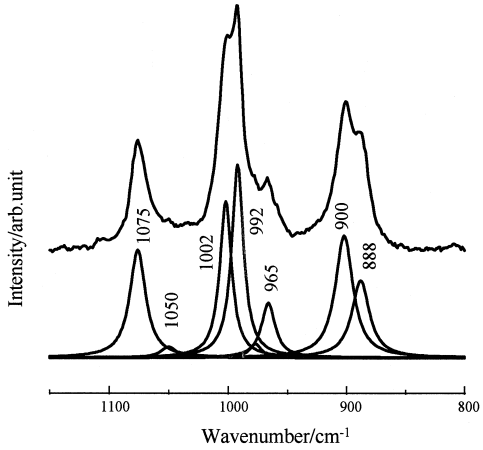

Fig. 3. Peak-shape analysis of the spectrum of Fig. 2c.

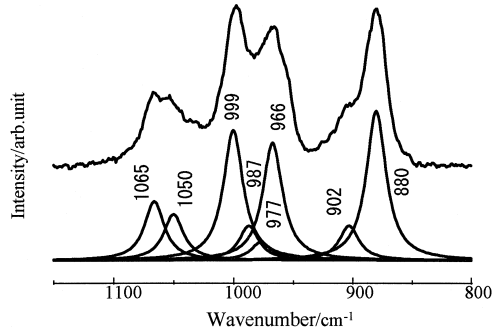

Fig. 4. Peak shape analysis of the spectra of well-exchanged catalyst (Fig. 2d) and separated peaks.

As described above, Schrader et al. [11] proposed that the bands at 992 and 900 cm^{-1} are attributed to the stretching vibrations of P–O_b–V. That at 1002 cm^{-1} is to the V=O vibration and that at 1075 cm^{-1} to P–O_a–V. The results in Fig. 2 and Table 3 indicate that the oxygen ions of P–O_b–V species exchange more preferentially than those of V=O and P–O_a–V. These indicate that oxygen insertion seems to take place on the vacancies corresponding to P–O_b–V positions. The bands at 1002 and 1076 cm^{-1} corresponding to V=O and P–O_a–V, respectively, are not exchanged at low ^{18}O exchange. This indicates that these are not the sites for reoxidation. Furthermore, the P–O_b–V oxygen ions seem to participate in the oxidation reactions since the ^{18}O exchange is very selective at the positions.

Fig. 2d shows the spectrum of β-$VOPO_4$ sufficiently exchanged with ^{18}O by repeating reduction by but-1-ene and reoxidation by $^{18}O_2$ for 5 times. All bands tend to exhibit line-broadening. Fig. 4 shows the peak shape analysis for the spectrum of Fig. 2d. The spectrum consists of the bands at 1065, 1050, 999, 987, 976, 966, 902, and 880 cm^{-1}. The band at 900 cm^{-1} shifts to 880 cm^{-1}. Those at 978 and 966 cm^{-1} are shifted from 999 (1002) and 988 (992) cm^{-1} respectively. The bands at 988 (992) and 902 have exchanged remarkably, which corresponds to P–O_b–V. The band at 999 cm^{-1} is the same as the one at 1002 cm^{-1} (as for ^{18}O exchange in Fig. 3 and in Table 3) which corresponds to V=O. Its intensity is not changed much in spite of the high ^{18}O exchange. The band at 1065 seems to be the same band, observed at 1075 cm^{-1} in Fig. 3 and Table 3, which is affected by replacement other oxygen

Table 3
Fractions obtained from peak-shape analysis over β-$VOPO_4$ catalyst exchanged with ^{18}O via redox reactions

Average ^{18}O% in β-$VOPO_4$	Exchange %			
	(P–O_b–V)		(V=O)	(P–O_a–V)
	$I_{888}/(I_{902}+I_{888})$	$I_{965}/(I_{992}+I_{965})$	$I_{977}/(I_{1002}+I_{977})$	
5[a]	8	7	0	0[c]
12	27	13	6	0
14	39	25	8	5
2[b]	8	5	0	0
5	0–10	6	0	0

[a,b] have the same meaning as in Table 2.
[c]A very small peak was observed at around 1050 cm^{-1} at low exchange region.

with ^{18}O in P tetrahedra. The band at 1050 cm^{-1} seems to be the shifted one such as $P–^{18}O_a–V$.

The shift intervals are determined as 26–22 cm^{-1} experimentally in the range from 1000 to 900 cm^{-1}. The V=O oxygen is not very active for oxidation reaction since the shift extent is low as described above.

3.4. Raman band shifts of β-$VOPO_4$ catalyst exchanged with ^{18}O by a catalytic oxidation

The catalyst oxygen ions were exchanged with ^{18}O via catalytic oxidation using but-1-ene and $^{18}O_2$. The average ^{18}O% are shown in Table 2. Fig. 5 shows the Raman spectra and the results of peak-shape analysis for the 2% sample. A small band at 967 and shoulder at ca. 880 cm^{-1} appear. The shift fractions for these bands are also shown in Table 3. It is concluded that the exchange, i.e., oxygen insertion, takes place on the $P–O_b–V$ vacancies rather than on V=O and $P–O_a–V$. The characteristic feature in this catalytic oxidation is the same as in the reduction–oxidation method as described above.

The average exchange % in the catalytic oxidation exhibits a smaller value though the conversions of but-1-ene are higher than those in the reduction–oxidation method (Table 3). The shift fractions of the 967 and 880 are somewhat smaller in the case of catalytic reactions. This seems to be because the catalytic oxidation takes place at the surface regions. As the product selectivities are nearly the same between in the reduction and catalytic oxidation, a redox mechanism should be operated here.

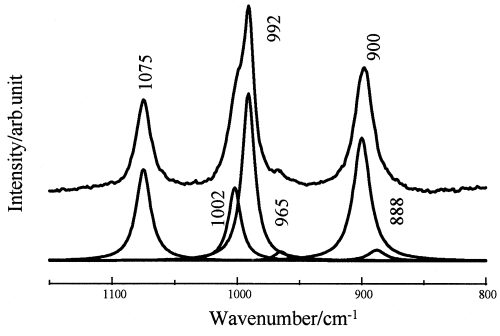

Fig. 5. Raman spectra of β-$VOPO_4$ exchanged with ^{18}O by a catalytic oxidation (see Table 2, 2%) of but-1-ene and its peak-shape analysis.

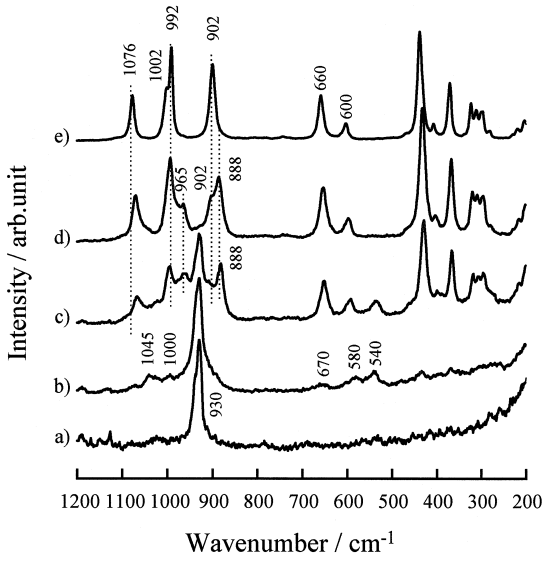

Fig. 6. Raman spectra of $(VO)_2P_2O_7$ oxidized by $^{18}O_2$ and $^{16}O_2$. (a) No oxidation, i.e. $(VO)_2P_2O_7$, (b) 23% oxidized by $^{18}O_2$, (c) 32% by $^{18}O_2$, (d) 81% by $^{18}O_2$, and (e) approx. 100% by $^{16}O_2$, i.e., β-$VOPO_4$ at 823–873 K and for 14–30 h.

3.5. Oxidation of $(VO)_2P_2O_7$ by $^{18}O_2$ and $^{16}O_2$ and their Raman spectra

It is well known that $(VO)_2P_2O_7$ is oxidized to β-$VOPO_4$ by O_2 above 823 K. $(VO)_2P_2O_7$ (Fig. 6a) has one strong Raman band at 930 cm^{-1} which is attributed to the vibration of P–O–P [9]. Fig. 6 shows the spectra after the oxidation of $(VO)_2P_2O_7$ with $^{18}O_2$ and $^{16}O_2$. The catalyst which has been oxidized by $^{16}O_2$ (Fig. 6e) exhibits bands at 1076, 1002, 992, and 900 cm^{-1}. This is the same spectrum as shown in Fig. 2a and characteristic for β-$VOPO_4$. The catalyst well-oxidized by $^{18}O_2$ (Fig. 6d) exhibits new bands at 965 and 888 cm^{-1} which were previously well observed and identified after reduction of β-$VOPO_4$ and reoxidation by $^{18}O_2$. The bands at 1076, 1002, 992, and 900 cm^{-1}

are also observed. With the catalyst oxidized by 32% with $^{18}O_2$, the bands at 963 and 880 cm^{-1} appears as shown in Fig. 6c. Fig. 7 shows the peak-shape analysis of it. The analysis indicates that the bands at 965 and 888 cm^{-1} grows more preferentially compared to other shifted bands. This suggests that ^{18}O oxygen is inserted preferentially to the position at P–O_b–V sites in the oxidation of $(VO)_2P_2O_7$. This feature is the same as reported by Lashier and Schrader [11]. They reported that the oxygen was inserted mainly at the position corresponding to the band at 900 cm^{-1}, i.e. new bands at 880 cm^{-1} appeared. The insertion of an oxygen seems to take place at the pair V^{4+} sites since the oxidation of $V^{4+} \rightarrow V^{5+}$ will occur there. Fig. 8 shows a structure model of $(VO)_2P_2O_7$ and β-$VOPO_4$. Some predictions are given. The separation of octahedral pair sites seems to accompany the oxygen insertion. The tetrahedral phosphate ions should be formed by the fission of pyrophosphate species. The ^{18}O does not enter P–O_a–V. This suggests that the oxygen ions of P–O_a–V come from those of square V and pyrophosphate species. The oxygen ions inserted from gaseous phase enter the P–O_b–V position as described above. When $(VO)_2P_2O_7$ is oxidized by gaseous oxygen, some $VOPO_4$ phases will be formed prior to the stable β-$VOPO_4$ phase formation. This is discussed below. Anyway, the Raman bands of β-$VOPO_4$

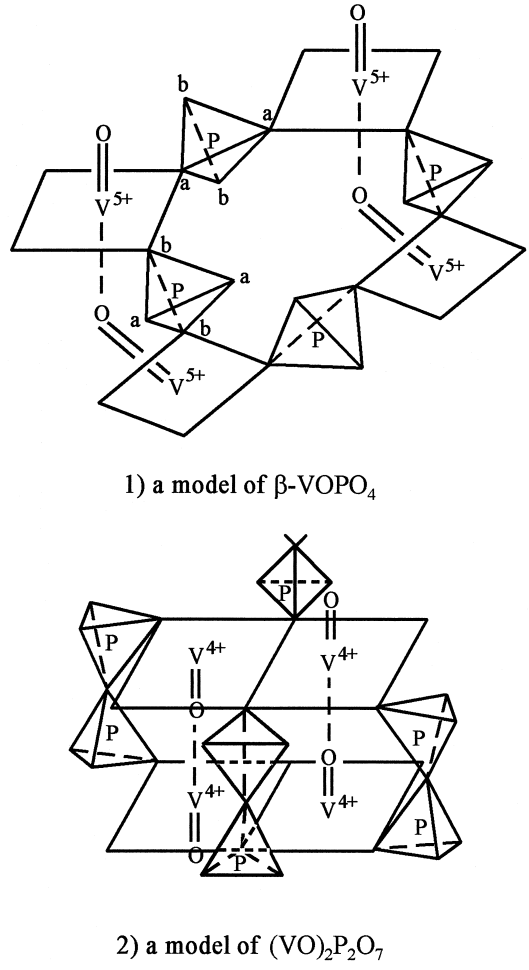

Fig. 8. Structure models of (1) β-$VOPO_4$ and (2) $(VO)_2P_2O_7$. In (1), (a) and (b) have the same meaning as those in Fig. 1. In (2), the oxygen ions of V^{4+} pair squares of $(VO)_2P_2O_7$ are all linked with pyrophosphate species, but some of them are omitted here.

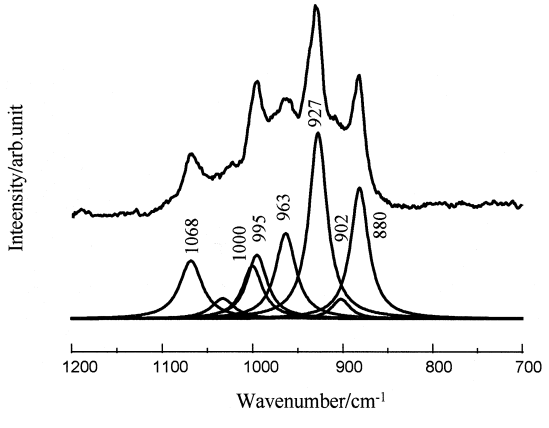

Fig. 7. Peak shape analysis of the spectrum of Fig. 6c.

are affected by V–O characters such as V–^{18}O and V–^{16}O. In this sense, the assignments in Table 1 by Schrader et al. will be better.

As shown in Fig. 6b, prior to β-$VOPO_4$ phase formation the different bands appear when the 23% of 18-oxygen uptake occurs over $(VO)_2P_2O_7$ catalyst. The new small bands at 1045, 1000, 670, 580 and 540 cm^{-1} appear. In using $^{16}O_2$, the small bands at 1040, 1000, 570, and 540 cm^{-1} were obtained at 17% of uptake. According to Koyano et al. [12,13], the bands at 1090, 937, and 590 cm^{-1} were obtained for

partially oxidized $(VO)_2P_2O_7$, which is named as a X_1 phase which will be responsible for maleic anhydride formation. In Ref. [14,15] the bands for δ-$VOPO_4$ are observed at 1090, 1075, 1020, 936, and 590 cm^{-1}. The bands by both workers are partly resemble. Abdelouhab et al. [14,15] proposed the structure of δ-$VOPO_4$ phase which is different from α_I, α_{II}, and γ-phases. The Raman bands by these workers [12–15] are different from those in this work. The surface oxidized compounds on $(VO)_2P_2O_7$ seem to depend on the experimental conditions reported in the studies. The new band appearance seems to originate from a new phase formation due to the oxygen insertion at V^{4+} pair sites prior to the stable phase formation of β-$VOPO_4$.

3.6. Redox features on β-$VOPO_4$ catalyst

The bands at 992 and 902 cm^{-1} of β-$VOPO_4$ shifted to lower frequencies with exchange of ^{18}O more preferentially in both reduction–oxidation and catalytic oxidation methods. This suggests that the P–O_b–V sites are responsible for reoxidation. In the first step of oxidation, the oxygen ions of P–O_a–V and V=O as well as P–O_b–V may react with but-1-ene possibly. After that, the anion vacancies may migrate to any position, and the ^{18}O insertion to P–O_a–V and V=O may occur as well as P–O_b–V. The oxygen insertion, however, takes place at P–O_b–V sites very selectively. It seems that the reaction with but-1-ene also occurs at P–O_b–V positions.

Lashier et al. [11] reported that the source of oxygen to furan and maleic anhydride is P–O_b–V while CO_2 will be formed on V=O. It seems that CO and CO_2 formations as well as oxidative dehydrogenation take place on P–O_b–V since the oxygen exchange occurred here very selectively in this work. The simple redox mechanism, i.e., the reduction of oxides and reoxidation of them at the same and homogeneous sites, has been discussed in the past [27]. As has been reported recently (see e.g. Ref. [28]), the reduction of oxide surface and its oxidation by gaseous oxygen occurs in different regions on the oxide catalysts such as Bi–Mo oxides. In this work, the oxidation takes place at restrict sites over β-$VOPO_4$ as far as the oxygen release and oxygen insertion are concerned.

Acknowledgements

We thank Prof. Hisashi Miyata for help in computer peak-shape analysis. We also thank Prof. Masakazu Anpo for using the Shimadzu Mass Spectrometer (GCMS QP 2000A).

References

[1] T. Ono, H. Numata, N. Ogata, J. Mol. Catal. A: Chemical 105 (1996) 31.
[2] T. Ono, N. Ogata, Y. Miyaryo, J. Catal. 161 (1996) 78.
[3] T. Ono, H. Numata, J. Mol. Catal. A: Chemical 116 (1997) 421.
[4] B.K. Hodnett, Catal. Rev. Sci. Eng. 27 (1985) 373.
[5] G. Centi, F. Trifiro, J.R. Ebner, V.M. Franchetti, Chem. Rev. 88 (1993) 55.
[6] E. Bordes, Catal. Today 1 (1987) 499.
[7] E. Bordes, Catal. Today 16 (1993) 27.
[8] I. Matsuura, A. Mori, M. Yamazaki, Chem. Lett. (1987) 1897.
[9] T.P. Moser, G.L. Schrader, J. Catal. 92 (1985) 216.
[10] T.P. Moser, G.L. Schrader, J. Catal. 104 (1987) 99.
[11] M.E. Lashier, G.L. Schrader, J. Catal. 128 (1991) 113.
[12] G. Koyano, T. Okuhara, M. Misono, Catal. Lett. 32 (1995) 205.
[13] G. Koyano, T. Saito, M. Misono, Chem. Lett. (1997) 415.
[14] F.B. Abdelouahab, R. Olier, N. Guilhaume, F. Lefebvre, J.C. Volta, J. Catal. 134 (1992) 151.
[15] F.B. Abdelouahab, J.C. Volta, R. Olier, J. Catal. 148 (1994) 334.
[16] Y. Zhang-Lin, M. Forissier, R.P. Sneeden, J.C. Vedrin, J.C. Volta, J. Catal. 145 (1994) 256.
[17] Y. Zhang-Lin, M. Forissier, J.C. Vedrin, J.C. Volta, J. Catal. 145 (1994) 267.
[18] R.N. Bhargava, R.A. Condrate Sr., Appl. Spectrosc. 31 (1977) 230.
[19] E. Bordes, P. Courtine, J. Catal. 57 (1979) 236.
[20] T. Shinoda, T. Okuhara, M. Misono, Bull. Chem. Soc. Jpn. 58 (1985) 2163.
[21] H. Igarashi, K. Tsuji, T. Okuhara, M. Misono, J. Phys. Chem. 97 (1993) 7065.

[22] H. Miyata, K. Fujii, S. Inui, Y. Kubokawa, Appl. Spectrosc. 40 (1986) 1177.
[23] H. Miyata, S. Tokuda, T. Yoshida, Appl. Spectrosc. 43 (1989) 522.
[24] R. Gopal, C. Calvo, J. Solid. State Chem. 5 (1972) 432.
[25] E. Bordes, P. Courtine, G. Pannetier, Ann. Chim. 8 (1973) 105.
[26] S.D. Ross, Inorganic Infrared and Raman Spectra, McGraw-Hill, New York, 1972.
[27] P. Mars, D.W. van Krevelen, Chem. Eng. Sci. Suppl. 3 (1954) 41.
[28] T.D. Snyder, G.C. Hill Jr., Catal. Rev. Sci. Eng. 31 (1989) 43.